

MANUFACTURE OF REFERENCE DEFECTS FOR NDE THROUGH HOT ISOSTATIC PRESSING

A.N. Sinclair, M. Graf, and V. daSilva

Department of Mechanical Engineering
University of Toronto
Toronto, Canada M5S 1A4

M.D.C Moles, M. Doleby, S. Kramer, and A.L. Allen

Metallurgical Research
Ontario Hydro, 800 Kipling Avenue
Toronto Canada M8Z 5S4

INTRODUCTION

Nondestructive Evaluation techniques such as eddy current or ultrasonics do not give a direct visual indication of the key characteristics of a flaw. Some form of signal interpretation is required in order to determine flaw type, size, and shape. One tool that is frequently employed in the field is the "reference defect"; in the case of ultrasonic testing, reference defects typically consist of notches and flat-bottom or side-drilled holes in a calibration block. Not only are these artificial sound reflectors used to aid in the interpretation of flaw signals, but they may also be used to check that the NDE equipment is working properly each time it is used.

Clearly, flat-bottom holes or square-cut notches bear no resemblance hairline cracks, inclusions or other real defects that might occur in an engineering component. This deficiency has become even more serious in recent years: the frequency range and sophistication of NDE equipment such as ultrasonic flaw detectors have made tremendous gains; the engineering community has seen increased use of materials such as ceramics and superalloys where even a minute defect could result in component failure. A specific example is the $Zr - 2.5\% Nb$ pressure tubes used in the CANDU nuclear reactor, where a lapping defect (visible only at ultrasonic frequencies above 50 MHz) was recently found to contribute to an in-service failure. Evaluation of such defects by comparison with signals from notches or drilled holes would be pointless. Even a calibration check of the equipment using such reference defects would be suspect, as drilled holes are clearly visible at frequencies down to a few megahertz, while detection of the flaws of interest requires much higher frequencies.

The objective of this study is to devise a method for implanting a reference defect in the wall of a CANDU pressure tube specimen in a repeatable manner. The flaw should be clearly visible in the 50 – 100 MHz band, but not readily visible below 30 MHz.

SUMMARY OF METHOD

The following list summarizes the key steps used in the manufacture of a reference defect in a CANDU pressure tube sample by hot isostatic pressing [1]:

1. Two pieces of CANDU pressure tube were cut, each 10.00 *cm* long. Physical properties of the Zr-2.5% Nb material are given in Table I, including density ρ , speed of longitudinal waves C_L , and acoustic impedance Z .
2. The wall thickness of one tube specimen was reduced by 50% by machining off the outer half of the wall material. The wall thickness of the other tube specimen was also reduced by 50%, but by machining off the *inner* half of the wall material.
3. Reference defects, consisting of thin foils and wires, were cut to have characteristic dimensions of about 2 *cm*. The materials used are listed in Table II, and their properties given in Table I.
4. Both tube sections were thoroughly cleaned and dried. The "defects" were then placed on the outer wall of the smaller diameter tube. A shrink-fitting procedure in which the inner tube was cooled with dry ice was then used to slide the two tubes together.
5. A rolling tool was then used at each end of the assembled tube specimen to force the wall of the inner tube into intimate contact with the outer tube. The rolling procedure did not affect any material at a distance greater than 1 *cm* from the ends of the specimen.
6. The assembled specimen was placed into an evacuated chamber to remove air from the interfacial area.
7. The ends of the tube were sealed shut by electron beam welding. This left the interfacial area under vacuum conditions.
8. The welded specimen was then subjected to hot isostatic pressing (HIP) at 900°C and 172 MPa (25,000 psi) for 4 hours. This was followed by an air cool.

Table I. Ultrasonic Properties of Materials

Material	density ρ (g/cm^3)	C_L ($mm/\mu s$)	$Z \left[10^6 \frac{kg}{m^2 s} \right]$
zirconium	6.4	4.65	30.1
steel	7.7	5.9	45
brass	8.4	4.40	37
tungsten	19.1	5.46	104
platinum	21.4	3.96	85
copper	8.9	4.70	42
glass	2.5	5.66	14
water	1.0	1.48	1.5

ULTRASONIC ANALYSIS

HIP Interface

Before examining the imbedded defects, an ultrasonic inspection was performed of the defect-free areas of the HIP'd tube, to confirm that it would respond to ultrasound in an essentially identical manner as a fresh pressure tube. A broadband (0 – 100 MHz) ultrasonic system was used to examine the HIP'd pressure tube specimen in a pulse-echo immersion configuration using compression waves. The interface between the two concentric tubes was not ultrasonically visible. (Destructive analysis with a scanning electron microscope

clearly showed metallurgical traces of the boundary line, but it was transparent to ultrasound in this frequency range.) A check of the attenuation coefficient α was also made in the HIP'd tube; this check was prompted by a concern that the HIP temperature cycle might have induced changes in the grain structure [2] that would affect α . The measurements confirmed that α for the HIP'd tube was not significantly different from that for a standard pressure tube sample.

Inspection of Thin Foils

The thin foil defects listed in Table 2 were ultrasonically examined over frequencies ranging from near zero to over 125 MHz, using high frequency probes manufactured by Panametrics. An immersion, normal beam configuration was used. Assuming plane waves with wave number k , the theoretical value of the reflection coefficient magnitude $|R|$ from a foil of thickness d is given by Brekhovskikh [3]:

$$|R| = \left[\frac{(Z_2^2 - Z_1^2)^2 \sin^2(k_2 d)}{(Z_2^2 + Z_1^2)^2 \sin^2(k_2 d) + 4Z_1 Z_2 \cos^2(k_2 d)} \right]^{\frac{1}{2}} \tag{1}$$

where subscript "1" refers to the pressure tube material, and subscript "2" refers to the defect material.

Table II. Defects in HIP'd Pressure Tube Specimen

Material	Geometry	Foil Thickness Wire Diameter (μm)
steel	foil	25.4
brass	foil	25.4
tungsten	wire	50.8
tungsten	wire	25.4
platinum	wire	12.7

Figure 1(a) shows the theoretical and experimental spectra of $|R(f)|$ for the 25.4 μm brass foil in the pressure tube. The experimental data were obtained by deconvolving the echo from the "defect" with the echo from a reference reflector - a glass plate. The experimental results show considerable noise, although the primary feature of interest - the marked dip in the spectrum at about 85 MHz - is seen in both the experimental and theoretical results. Note that this defect does not meet the objective of being visible only at high frequencies. In fact, this defect was distinctly visible even for probes with a central frequency in the 5-10 MHz range.

Figure 1(b) shows the theoretical and experimental spectra for the same brass foil, but now in water instead of zirconium alloy. The noise level for the experimental spectrum is much lower than was seen in Figure 1(a). The relatively high noise level of Figure 1(a) can

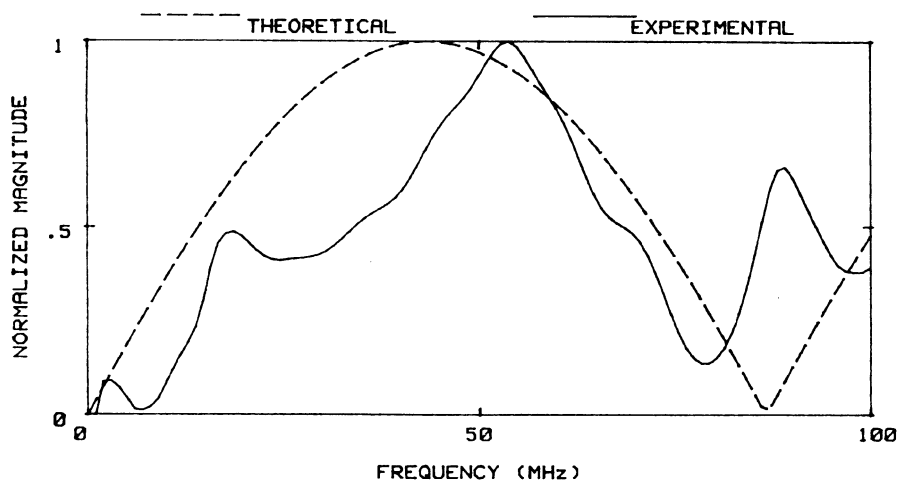


Fig. 1(a). Spectrum of $|R|$ from a 25 μm thick brass foil in Zr.

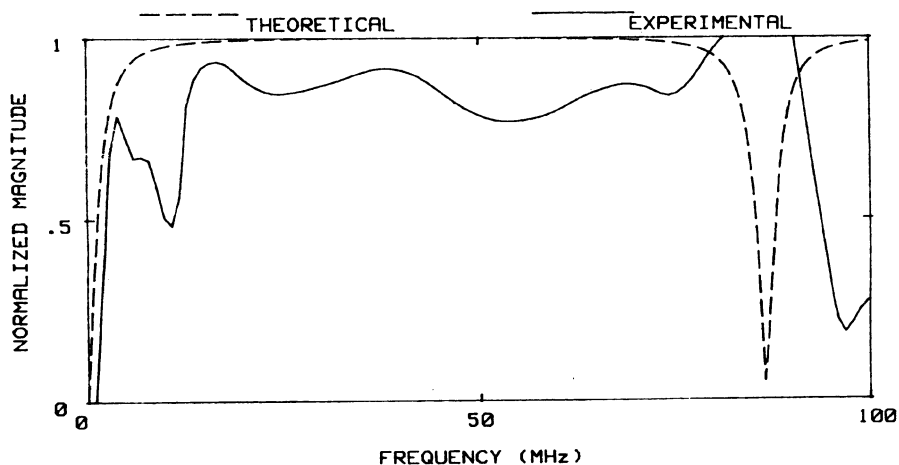


Fig. 1(b). Spectrum of $|R|$ from a 25 μm thick brass foil in water.

be attributed to the curved surface of the tube specimen (which would refract the sound beam and distort its planar nature), surface roughness, grain structure which would lead to sound diffraction, and interdiffusion of the brass shim with the Zr material - a phenomenon that showed up clearly in a SEM picture of the defect cross section.

Inspection of Thin Wires

The spectrum of the deconvolved signal reflected back by a thin wire is illustrated by Figure 2. Figure 2(a) shows the theoretical and experimental spectra $|R(f)|$ (in arbitrary units) for a $25.4\text{ }\mu\text{m}$ tungsten wire in the HIP'd tube specimen; Figure 2(b) shows the corresponding spectra for the tungsten wire in water. The theoretical curves of Figure 2 were determined using an asymptotic Bessel function expansion to a solution of the wave equation in cylindrical co-ordinates⁴.

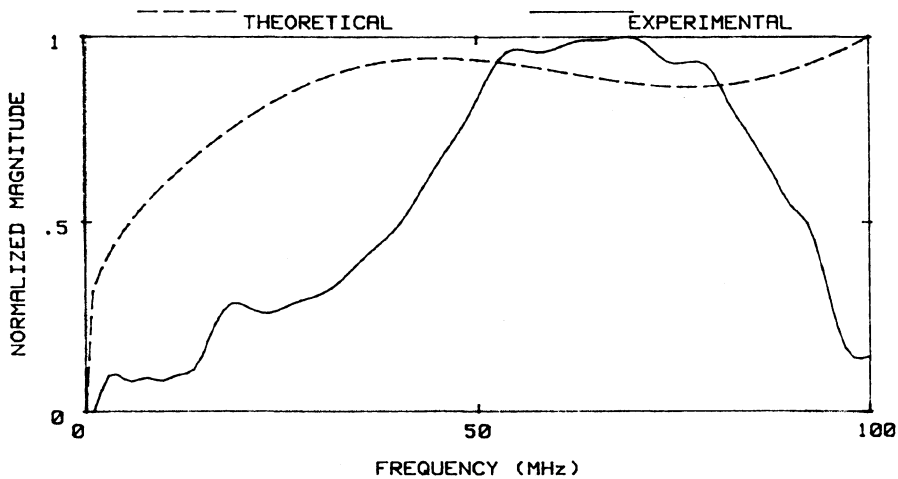


Fig. 2(a). Spectrum of $|R|$ from a $25\text{ }\mu\text{m}$ diameter tungsten wire in Zr.

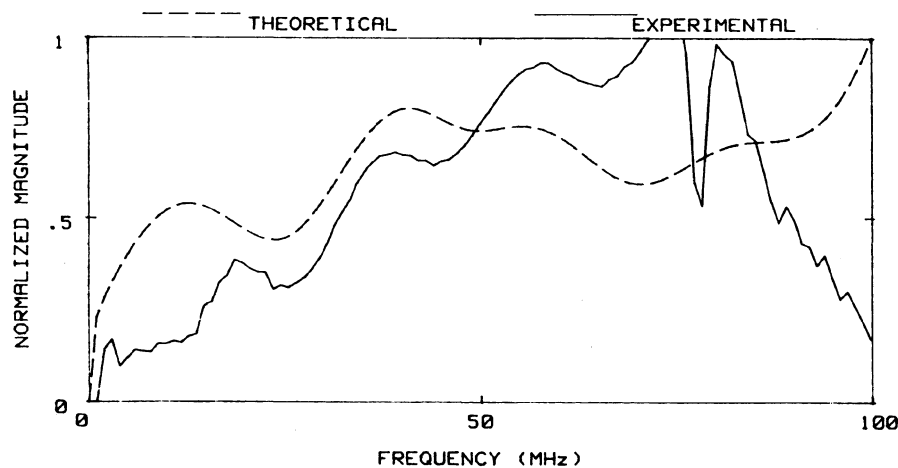


Fig. 2(b). Spectrum of $|R|$ from a $25\text{ }\mu\text{m}$ diameter tungsten wire in water.

There is reasonable qualitative agreement between the two spectra of Figure 2(b), indicating that the approximate solution to the wave equation is adequate for these purposes. The only major difference in the two graphs is the pronounced dip in the experimental spectrum at 80 MHz; this dip is completely absent in the approximate theoretical curve. The reason for the discrepancy is believed to be that the mathematical model does not account for the induced wave that travels around the circumference of the wire. Apart from this discrepancy, it is seen that the mathematical model does characterize the frequency dependence of $|R|$. Figure 2(b) indicates that the spectrum of $|R|$ for a wire in water is somewhat complicated compared to that shown for a shim in Figure 1(b).

Figure 2(a) shows that the measured spectrum for $|R(f)|$ corresponding to a wire in a Zr tube exhibits considerable noise. These observations indicate that there is little advantage in using thin wires as opposed to thin shims (or foils) as defects.

ANALYSIS AND DISCUSSION

The results given in the previous section do not meet the objective of producing a defect that is visible only at high ultrasonic frequencies. Figures 3 and 4, respectively, illustrate how the thickness and impedance of a foil-like defect affect $|R(f)|$. From these two figures, it is clear that the optimum solution would be to select a defect whose impedance Z is markedly different from that of $Zr-2.5\% Nb$, as this will give a better signal-to-noise ratio. Once Z and the longitudinal velocity C_L of the defect have been decided, the shim thickness can be selected using a graph such as that shown in Figure 4. The ideal thickness would feature a value of $|R|$ that is steeply rising with frequency at the desired cutoff value of 50 MHz. These arguments suggest that the foil-like defects will need to be much thinner than those discussed in the previous section. Appropriate specimens are currently under construction. Using Eq. (1), the spectrum of $|R(f)|$ was determined for the planned defects in the ne tube specimens; the results are shown in Figure 5. A comparison with Figures 1(a) and 2(a) indicates that this new set of defects should be better suited to meeting the objective of being visible only at frequencies that are well above the common range for ultrasonic NDE.

It should be noted that the most dangerous defects in a CANDU pressure tube are those that break the surface, because cracks originating at such defects tend to have comparatively large stress intensity factors. Such defects can be simulated by the HIP process by implanting the "defect" at an angle; the HIP'd specimen is then milled down to expose the tip of the imbedded "defect".

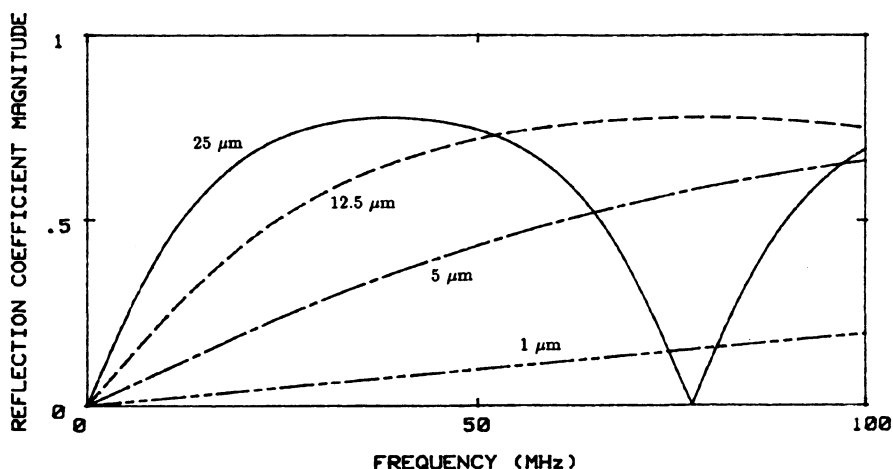


Fig. 3. Theoretical spectra of $|R|$ from Platinum foils in Zr.

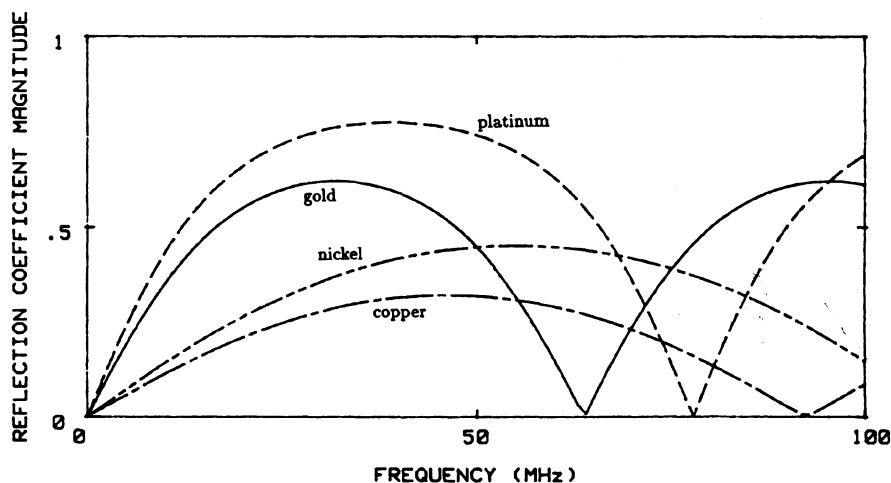


Fig. 4. Theoretical spectra of $|R|$ from 25 μm thick foils in Zr.

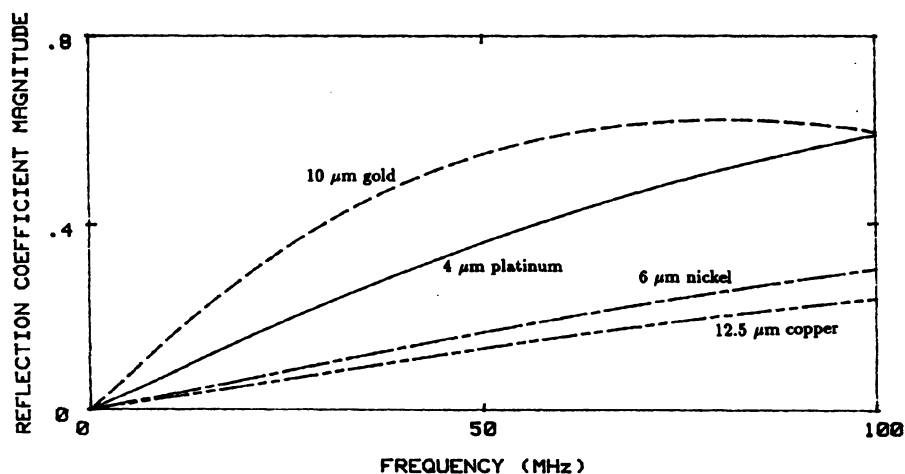


Fig. 5. Theoretical spectra of $|R|$ from foils in second generation of HIP'd pressure tubes.

SUMMARY AND CONCLUSIONS

1. A HIP procedure has been developed for implanting foils and thin wires in a Zr-2.5% Nb CANDU pressure tube wall. The HIP parameters of 900°C and 172 MPa for 4 hours were found to be appropriate for joining two sections of a pressure tube specimen such that ultrasound can not detect their interface.
2. The spectra of $|R(f)|$ obtained from the defects in the HIP'd pressure tube specimen were found to be in qualitative agreement with analytical predictions. Considerable noise was evident in the experimental results; this noise was significantly diminished by analyzing the same defect shapes in a water immersion configuration.

3. The defects tested to date were too thick to meet the objective of being almost invisible to ultrasound signals of 1 *MHz*. Mathematical modeling indicated the degree of thickness reduction required for various defect materials in order to meet the frequency dependence objective.
4. New specimens are currently being assembled with foil-like "defects" ranging from 4 – 12.5 μm thickness, and wire-like defects ranging from 8 – 25.4 μm diameter. The mathematical model indicates these defects should give comparatively little ultrasonic reflection below approximately 50 *MHz*.

ACKNOWLEDGEMENTS

This project was funded by a contract from Ontario Hydro, a grant from the Ontario Ministry of Colleges and Universities, and grants from the Natural Sciences and Engineering Research Council of Canada. The hot isostatic pressing was performed by D. Morphy of the National Research Council, Ottawa.

REFERENCES

1. M.A. Graf, "The Manufacture and Analysis of a Reference Defect for High Frequency Ultrasonic Inspections of CANDU Pressure Tubes", B.A.Sc. Thesis, University of Toronto, 1990.
2. B. Cox, University of Toronto, private communication, 1989.
3. L.M. Brekhovskikh, "Waves in Layered Media", Academic Press, New York, 1980.
4. P.M. Morse, "Theoretical Acoustics", Chapter 8, McGraw-Hill, 1968.
D.O. Northwood, I.M. London, and L.E. Bahen, "Elastic Constants of Zirconium Alloys", Journal of Nuclear Materials, Vol. 55, pp 299-310, 1975.